Neuroimaging Pharmacopoeia

Daniel Thomas Ginat
Juan E. Small
Pamela Whitney Schaefer
Editors

Second Edition

Springer

Neuroimaging Pharmacopoeia

Daniel Thomas Ginat • Juan E. Small
Pamela Whitney Schaefer
Editors

Neuroimaging Pharmacopoeia

Second Edition

Springer

Editors
Daniel Thomas Ginat
Department of Radiology
University of Chicago
Chicago, IL, USA

Juan E. Small
Diagnostic Radiology
Lahey Hospital and Medical Center
Burlington, MA, USA

Pamela Whitney Schaefer
Department of Neuroradiology
Massachusetts General Hospital
Boston, MA, USA

ISBN 978-3-031-08773-8 ISBN 978-3-031-08774-5 (eBook)
https://doi.org/10.1007/978-3-031-08774-5

© Springer Nature Switzerland AG 2022
This work is subject to copyright. All rights are reserved by the Publisher, whether the whole or part of the material is concerned, specifically the rights of translation, reprinting, reuse of illustrations, recitation, broadcasting, reproduction on microfilms or in any other physical way, and transmission or information storage and retrieval, electronic adaptation, computer software, or by similar or dissimilar methodology now known or hereafter developed.
The use of general descriptive names, registered names, trademarks, service marks, etc. in this publication does not imply, even in the absence of a specific statement, that such names are exempt from the relevant protective laws and regulations and therefore free for general use.
The publisher, the authors, and the editors are safe to assume that the advice and information in this book are believed to be true and accurate at the date of publication. Neither the publisher nor the authors or the editors give a warranty, expressed or implied, with respect to the material contained herein or for any errors or omissions that may have been made. The publisher remains neutral with regard to jurisdictional claims in published maps and institutional affiliations.

This Springer imprint is published by the registered company Springer Nature Switzerland AG
The registered company address is: Gewerbestrasse 11, 6330 Cham, Switzerland

Contents

Part I

Drugs and Alcohol

Tobacco

1

Michael C. Veronesi and Daniel Thomas Ginat

1.1 Uses

Although tobacco use is legal, it is not recommended or prescribed for any therapeutic or medicinal purposes. It is smoked or chewed for recreational use as a potent temporary stimulant and mood elevator.

1.2 Mechanism

Nicotine, the primary active compound in cigarettes, is considered one of the most addictive of all substances because of its rapid onset and offset effects on the brain's dopamine reward systems. Inhaled nicotine can distribute in the brain within 10 s of inhalation but lasts mere seconds, causing a powerful urge for more. Of note, the long-term devastating sequela from smoking as it relates to neurologic disease are only partially explained by nicotine. Aside from nicotine, tobacco contains over 6000 other chemical compounds. In particular, polycyclic aromatic hydrocarbons and the tobacco-specific nitrosamine 4-(methylnitrosamino)-1-(3-pyridyl)-1-butanone have been implicated as the major carcinogens associated with cigarette smoking. Additional details regarding the mechanisms of action for specific conditions are discussed in subsequent sections.

1.3 Imaging Findings

Tobacco use is the leading cause of preventable death in the USA. An estimated 400,000 deaths or nearly one of every five deaths in the USA is associated with adverse conditions caused by smoking each year. Nearly every organ system is affected by cigarette smoking. The associated manifestations of cigarette smoking from a neuroimaging standpoint include the direct link between smoking and large vessels and lacunar infarcts, chronic small vessel ischemic disease, cerebral aneurysms, cerebral venous thrombosis, head and neck cancer of the squamous type, lung cancer metastases to the brain, and Warthin tumors.

1.3.1 Stroke

Compared with nonsmokers, cigarette smoking is estimated to increase the risk of stroke by two to fourfold. Of note, stroke is the third leading cause of death in the USA with significant comorbidity in survivors. Mechanisms by which primary and second-hand tobacco smoke exposure increase the risk of stroke and heart disease

M. C. Veronesi · D. T. Ginat (✉)
Department of Radiology, University of Chicago, Chicago, IL, USA
e-mail: dtg1@uchicago.edu

© Springer Nature Switzerland AG 2022
D. T. Ginat et al. (eds.), *Neuroimaging Pharmacopoeia*,
https://doi.org/10.1007/978-3-031-08774-5_1

include carboxyhemoglobinemia, increased platelet aggregation, increased fibrinogen levels, reduced HDL cholesterol, and direct toxic effects of compounds such as 1,3-butadiene, a vapor phase constituent of environmental tobacco smoke that has been shown to accelerate atherosclerosis. Indeed, atherosclerosis and formation of both occlusive and embolic thrombi are the major causes of cerebrovascular accidents. Smoking is also associated with lacunar infarcts and chronic small vessel ischemic disease. Smoking cessation results in a considerable reduction in stroke risk.

On conventional angiography, CTA or MRA, atherosclerosis manifests as luminal narrowing that may be associated with calcifications. Acute embolic thrombus is suggested by intraluminal high attenuation on non-contrast CT, such as the hyperdense MCA sign, and manifests as an abrupt termination of the artery with absence of flow distally on CTA, MRA, or conventional angiography (Fig. 1.1). Hyperacute infarcts are often unapparent on non-contrast CT, but acute and early subacute infarcts can appear as areas of hypoattenuation with loss of gray white matter differentiation and swelling. MRI with diffusion-weighted imaging is more sensitive for detecting early infarcts, which appear as areas of high T2 signal and restricted diffusion (Fig. 1.2). Besides smoking, other causes and risk factors for stroke include hypertension, hypercholesterolemia, diabetes, use of other drugs, such as cocaine and amphetamines (refer to Chaps. 5 and 6), dissection (Fig. 1.3), and vasculitis, such as lupus or Takayasu arteritis (Fig. 1.4). In addition to large territorial infarcts, smokers are prone to more extensive small vessel ischemic disease, which can manifest as areas of high T2 signal in the cerebral white matter (Fig. 1.5).

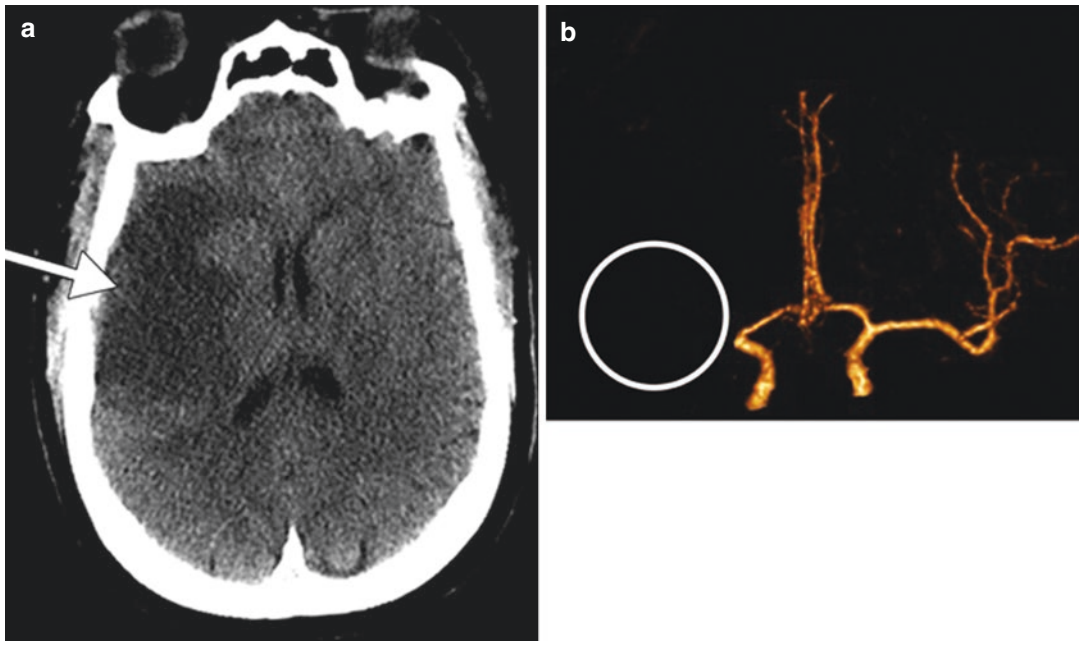

Fig. 1.1 Embolic infarct. This smoker presented with acute left hemiplegia. Non-contrast axial CT image (**a**) shows a hypoattenuation within the right MCA territory (*arrow*). 3D CTA image (**b**) shows occlusion of the right MCA (expected location *encircled*)

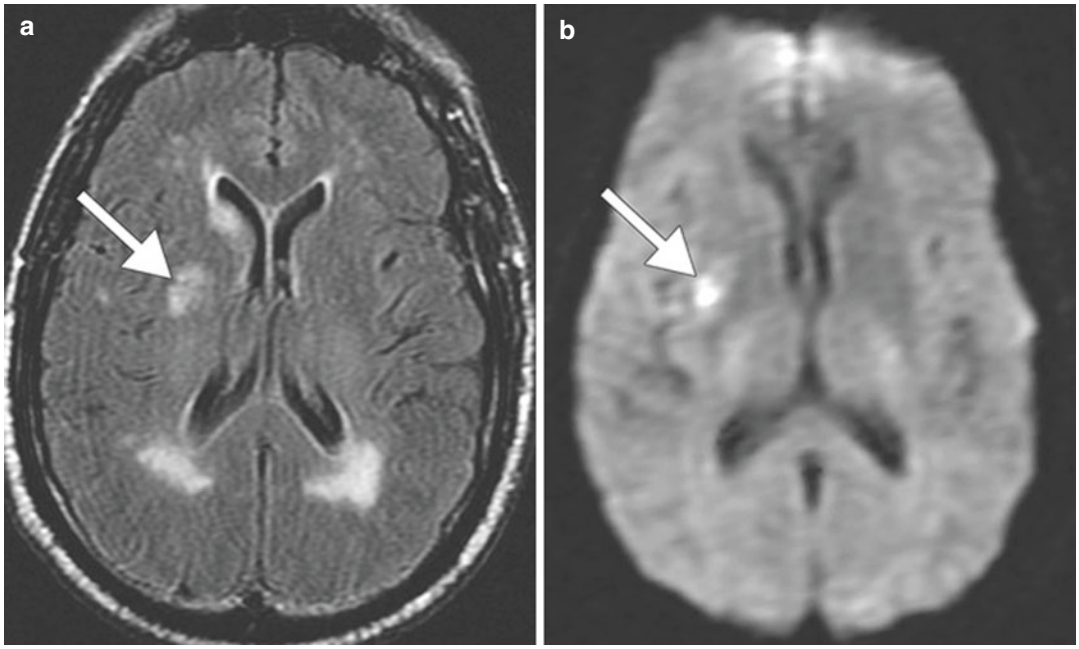

Fig. 1.2 Lacunar infarct and small vessel ischemic disease. The patient is a smoker who presented with acute neurological deficits. Axial T2-weighted FLAIR (**a**) and DWI (**b**) images show a recent right basal ganglia lacunar infarct (*arrows*). There is also diffuse, confluent periventricular white matter T2 hyperintensity as well as mild scattered, punctate subcortical white matter T2 hyperintense foci without corresponding restricted diffusion, which is consistent with chronic small vessel ischemic disease

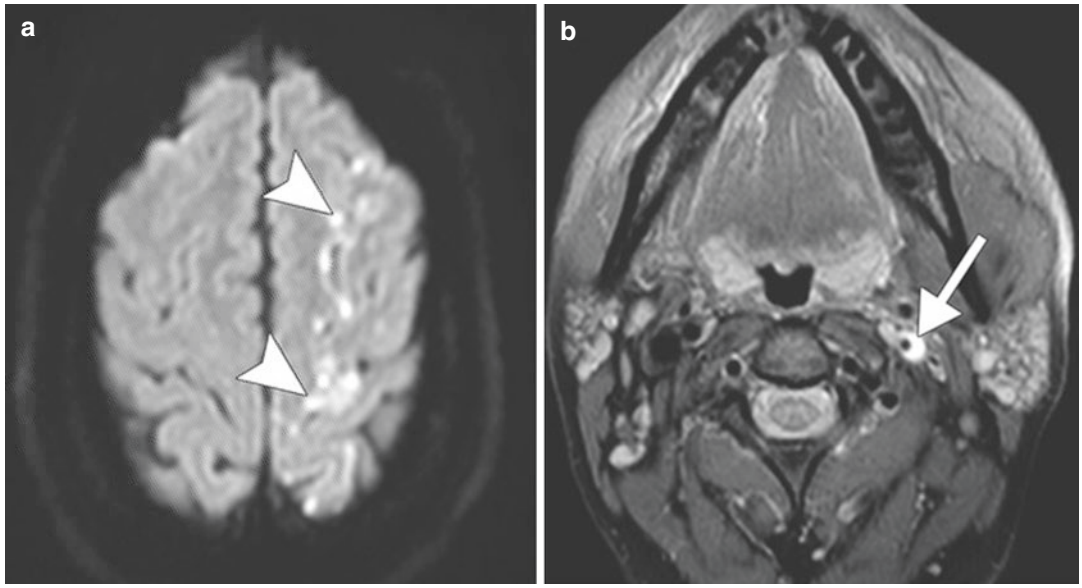

Fig. 1.3 Carotid dissection. Axial DWI (**a**) shows restricted diffusion in the left ACA-MCA watershed territory (*arrowheads*). The axial fat-suppressed T1 MRA (**b**) shows hyperintensity surrounding the narrow left internal carotid artery flow void, compatible with intramural hemorrhage (*arrow*)

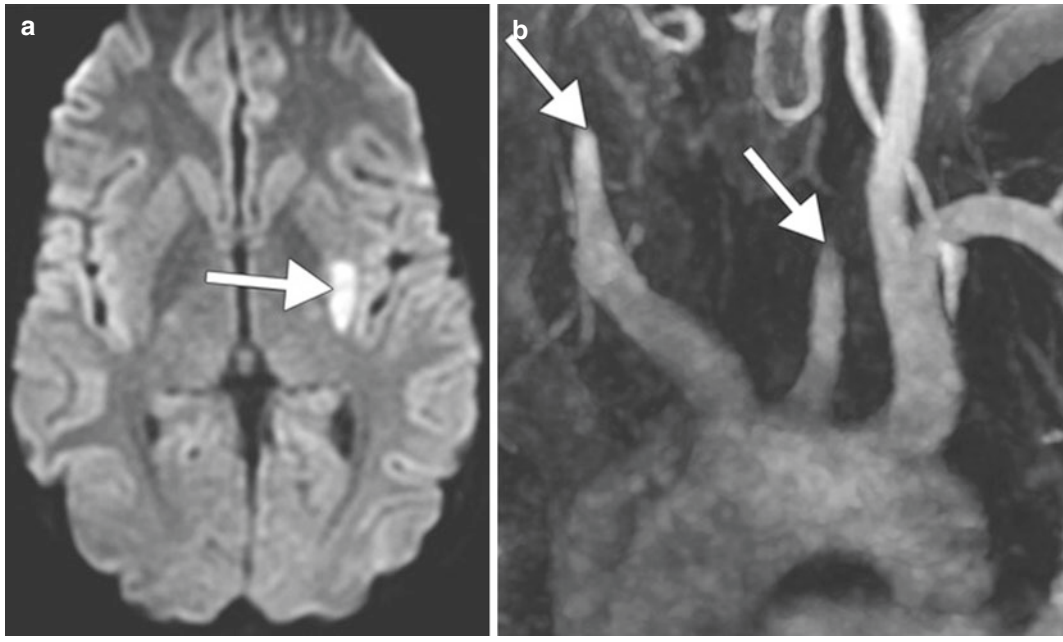

Fig. 1.4 Takayasu arteritis. Axial DWI (**a**) shows a focus of restricted diffusion in the left external capsule (*arrows*). MIP MRA (**b**) shows lack of flow-related enhancement beyond the proximal common carotid arteries bilaterally (*arrows*)

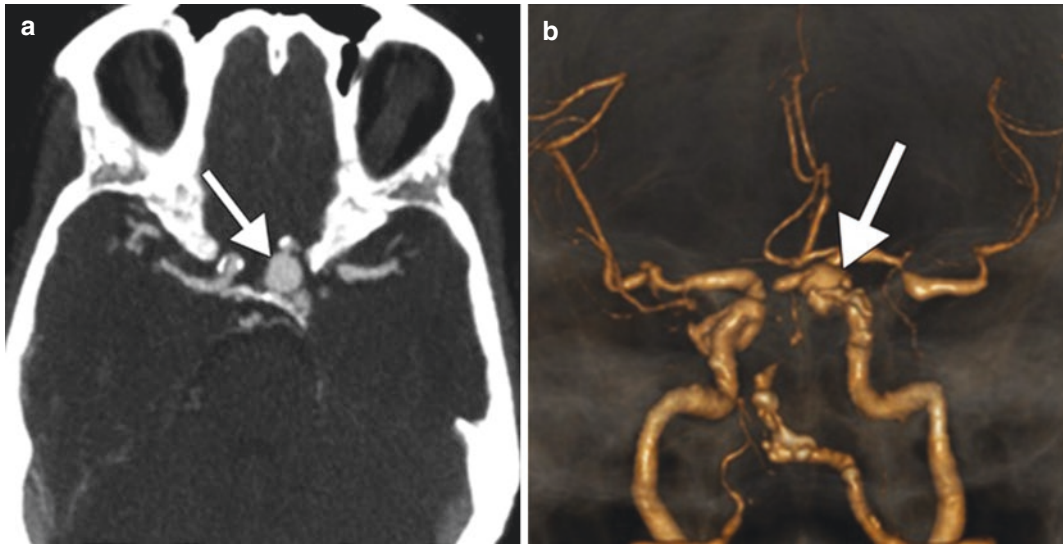

Fig. 1.5 Cerebral aneurysm. A former 20-pack-year smoker underwent evaluation for a suspected stroke. Axial (**a**) and 3D volume rendered (**b**) CTA images show a left paraclinoid internal carotid artery saccular aneurysm (*arrow*). There is also extensive atherosclerotic narrowing of the cerebral vasculature noted in both the anterior and posterior circulation bilaterally

1.3.2 Cerebral Aneurysm

Besides smoking, additional risk factors that predispose to aneurysm formation include fenestrated arteries (Fig. 1.6), fibromuscular dysplasia, neurofibromatosis, alpha-1-antytripsyn deficiency, and connective tissue disorders, such as Ehlers-Danlos syndrome and Marfan's syndrome and polycystic kidney disease. Otherwise, the differential diagnosis of a cerebral aneurysm on radiologic imaging includes an infundibulum (usually manifests as a triangular dilatation with the vessel arising from the apex that measures less than 2 mm), pseudoaneurysm, and mycotic aneurysm (Fig. 1.7).

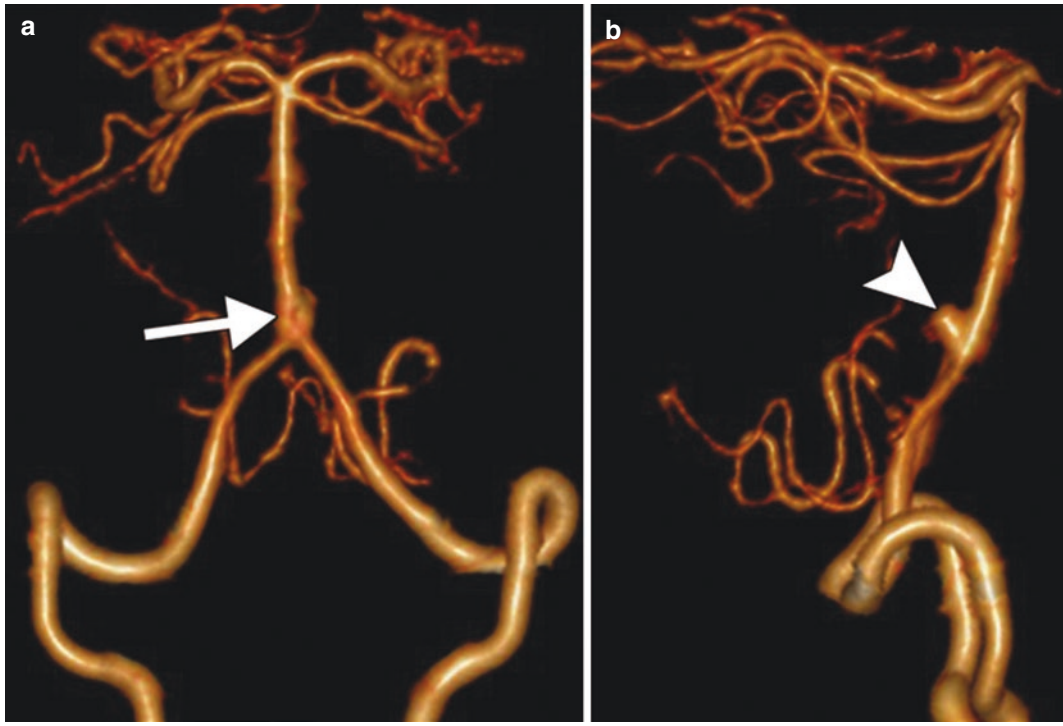

Fig. 1.6 Arterial fenestration. Frontal projection 3D volume rendered CTA image (**a**) shows a fenestration of the proximal basilar artery (*arrow*). Lateral projection 3D volume rendered CTA image (**b**) shows a dorsally oriented aneurysm arising from the caudal aspect of the fenestration (*arrowhead*)

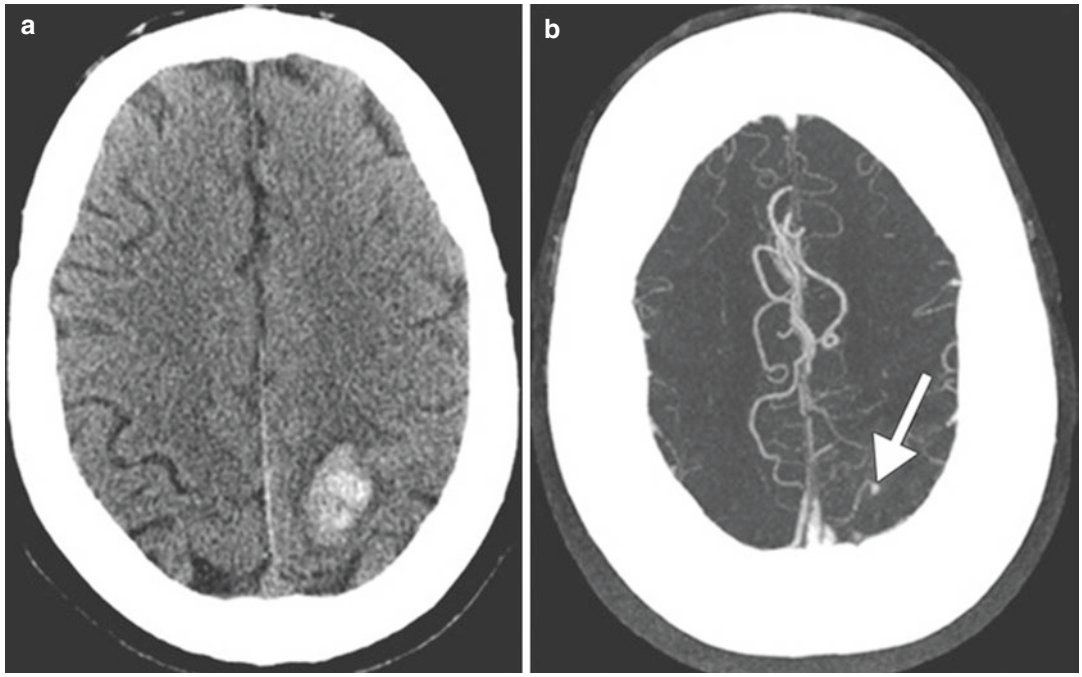

Fig. 1.7 Mycotic aneurysm. Axial CT image (**a**) shows left peri-rolandic hemorrhage. Axial MIP CTA image (**b**) shows a small outpouching arising from a cortical artery (*arrow*)

1.3.3 Cerebral Venous Thrombosis

Secondary polycythemia due to chronic smoking is a risk factor developing cerebral venous thrombosis. Refer to the L-asparaginase and oral contraceptives chapters (Chaps. 21 and 47) for examples of venous thrombosis on imaging.

1.3.4 Head and Neck Cancer, Squamous Cell Carcinoma

Tobacco smoking, along with alcohol, is well established as the dominant risk factor for head and neck squamous cell carcinoma (HNSCC). This risk is correlated with the intensity and duration of tobacco use and is synergistic with concomitant alcohol consumption. There are more than 60 recognized compounds in tobacco that have a specific carcinogenic potential. In particular, nitrosamines and polycyclic hydrocarbons can alter the molecular profile of an individual and causes mutations. Nicotine, originally thought only to be responsible for tobacco addiction, is also involved in tumor promotion and progression with antiapoptotic and indirect mitogenic properties. Other factors that can increase the risk of HNSCC include HPV infection and certain occupational exposures. Imaging with contrast-enhanced CT and MRI allows depiction of the anatomy of the larynx and submucosal tumor extension.

Dual-energy CT improves the diagnostic performance and interobserver reproducibility of evaluations of laryngeal cartilage invasion by squamous cell carcinoma. CT, MRI, and PET-CT

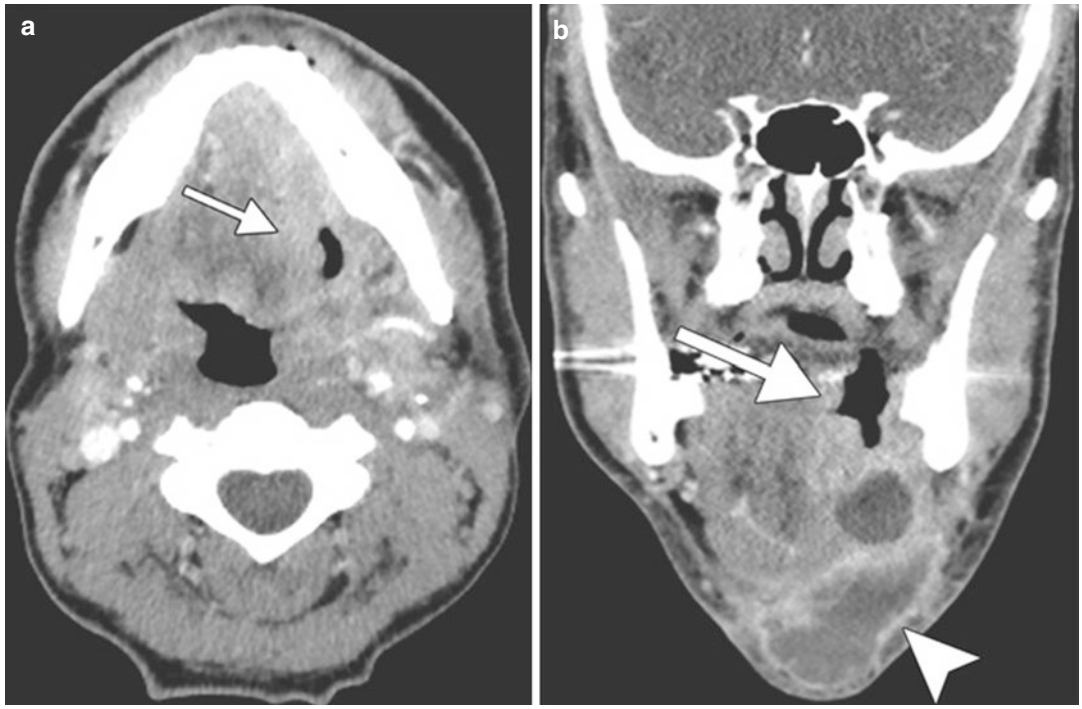

Fig. 1.8 Oral squamous cell carcinoma in a 30-pack-year male smoker. Axial (**a**) and coronal (**b**) post-contrast CT images show an ulcerating mass in the left floor of the mouth and oral tongue (*arrows*) with associated submental necrotic cervical lymphadenopathy (*arrowhead*)

also provide information regarding cervical nodal disease, systemic metastases, and synchronous malignancies.

On CT or MRI, head and neck squamous cell carcinomas often manifest as ill-defined enhancing masses. Aggressive features of HNSCC include tissue invasion and necrosis (Fig. 1.8). The most common sites of head and neck squamous cell cancer are the floor of the mouth, tongue, soft palate, anterior tonsillar pillar, and retromolar trigone. In addition to locoregional spread, HNSCC can metastasize to distant organs hematogenously, most commonly to the lungs and bones. Metastasis to the brain is infrequent, but carries a poor prognostic outcome (Fig. 1.9). Besides smoking, alcohol (refer to Chap. 2), betel nuts (refer to Chap. 8), and HPV are the other major risk factors for head and neck squamous cell carcinoma. Interestingly, HPV-positive squamous cell carcinomas generally have a more favorable prognosis and tend to have tumors that are relatively well-defined and large cystic nodal metastases (Fig. 1.10). Otherwise, the differential for other malignant cancers in the head and neck include thyroid cancer, lymphoma, salivary gland cancer, and sarcoma. Furthermore, head and neck abscesses can sometimes resemble necrotic or ulcerated head and neck squamous cell carcinomas and nodal metastases (Fig. 1.11).

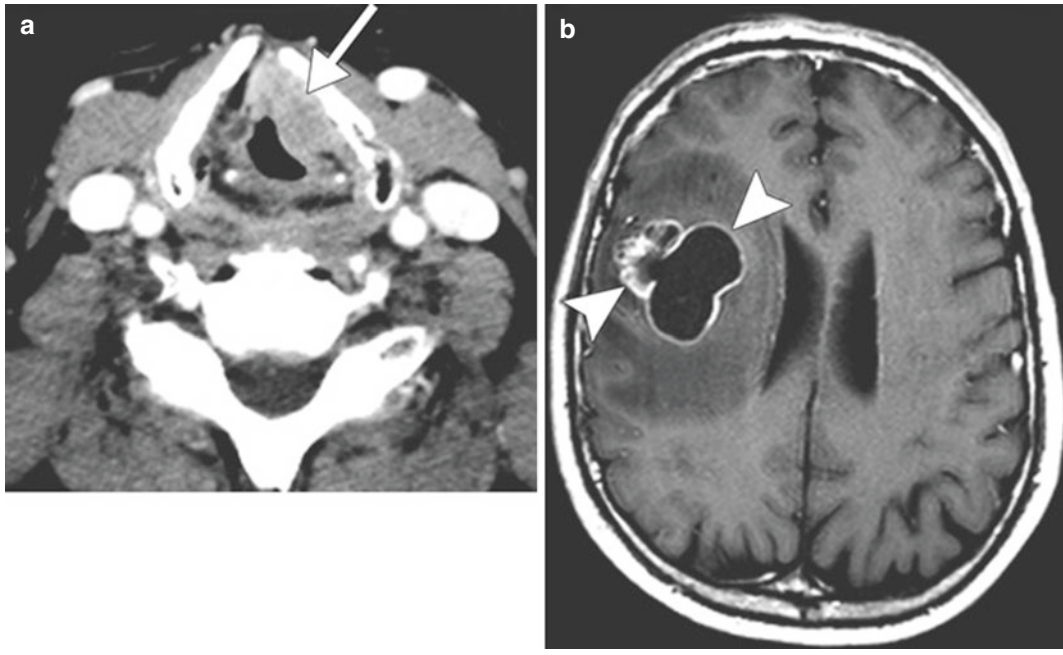

Fig. 1.9 Laryngeal squamous cell carcinoma with brain metastasis. This 25-pack-year smoker had been recently diagnosed with laryngeal squamous cell carcinoma when he developed generalized seizures. Axial CT image (**a**) shows a left vocal cord mass (*arrow*) that also involves the paraglottic fat and anterior commissure. Post-contrast T1-weighted MRI image (**b**) demonstrates a heterogeneous metastatic lesion in the right frontal lobe (*arrowheads*)

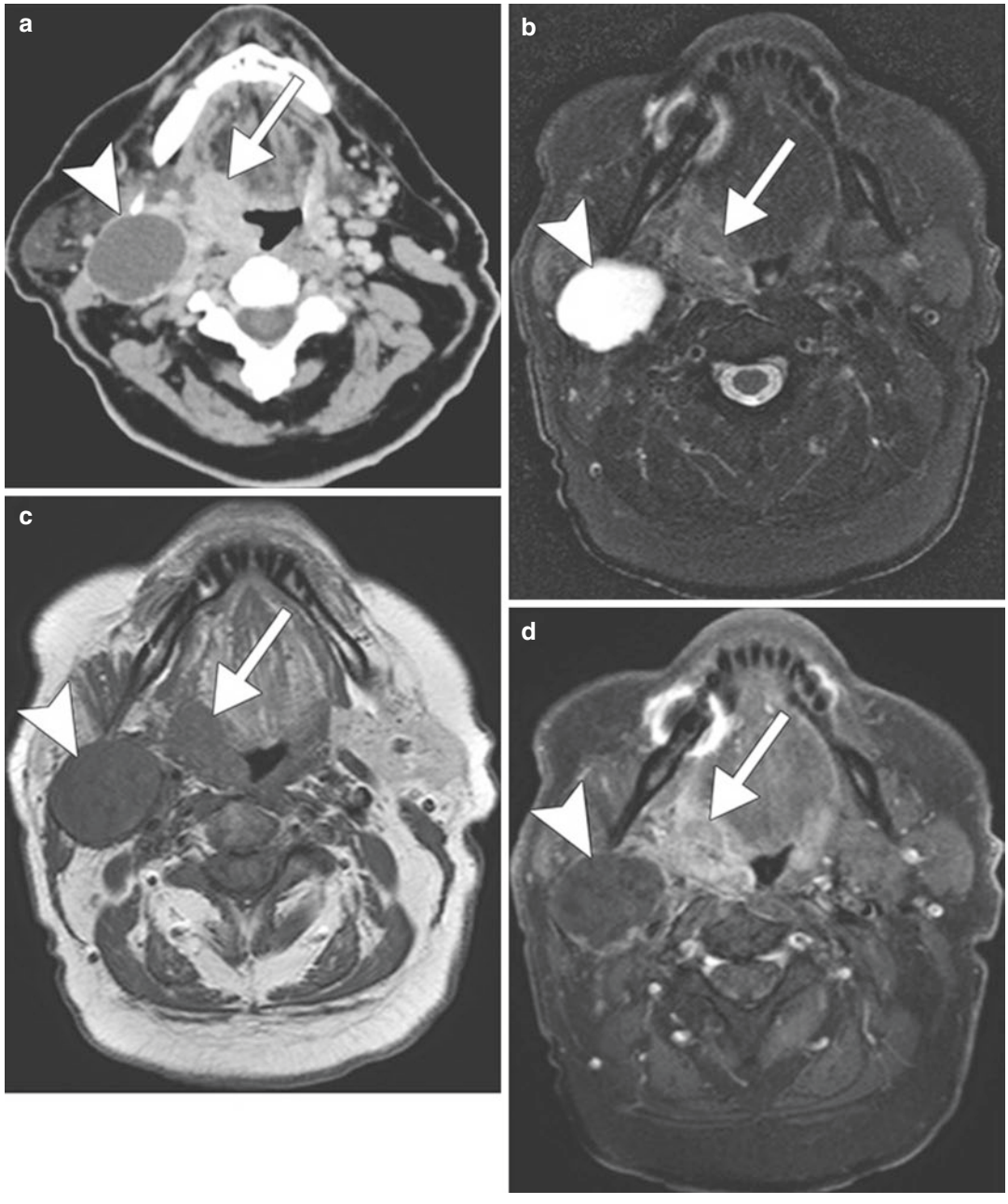

Fig. 1.10 HPV-positive squamous cell carcinoma. Axial CT (**a**) and axial fat-suppressed T2-weighted (**b**), axial T1-weighted (**c**), and axial fat-suppressed post-contrast T1-weighted (**d**) images show a relative well-demarcated right palatine tonsil tumor (*arrows*) and a large metastatic lymph node with cystic necrosis (*arrowheads*)

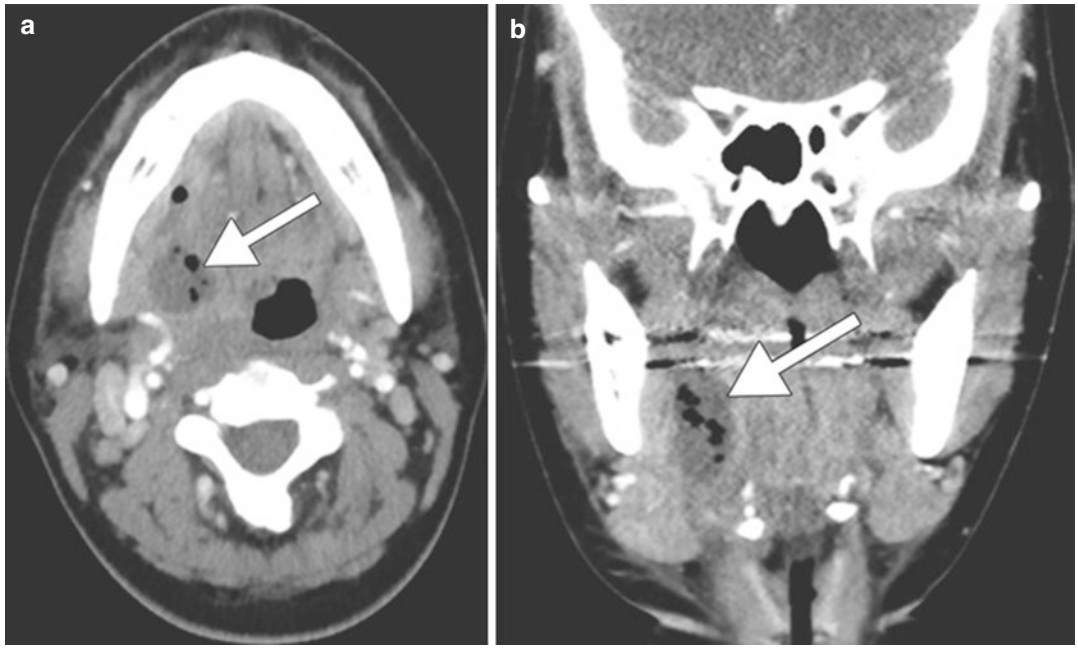

Fig. 1.11 Floor of mouth abscess. Axial (**a**) and coronal (**b**) post-contrast CT images show a fluid collection with internal air in the right floor of the mouth (*arrows*) in a patient with mouth pain and fever

1.3.5 Brain Metastases

In addition to HNSCC, smoking has been shown to be a risk factor for the formation of several other types of cancers, including lung cancer, acute myeloid leukemia, bladder cancer, cervical cancer, renal cancer, esophageal cancer, gastric cancer, pancreatic cancer, and colorectal cancer. The majority of these cancers have at least some potential for metastasizing to the brain, which is the most feared complication of systemic malignancies. If no one smoked, one of every three cancer deaths in the USA would be avoided. Lung cancer has the highest association with smoking, causing an estimated 90% of all lung cancer deaths in men and 80% of all lung cancer deaths in women, and is the most common cancer that metastasizes to the brain. Nicotine-derived nitrosamine ketone (NNK) has been identified as a potent procarcinogen specific to the development of lung cancer. The two categories of lung cancer metastases to the brain consist of small cell lung carcinoma (Fig. 1.12) and non-small cell lung carcinoma (NSCLC), such as adenocarcinoma (Fig. 1.13). MRI with contrast is the gold standard for evaluation of brain metastases. Lung

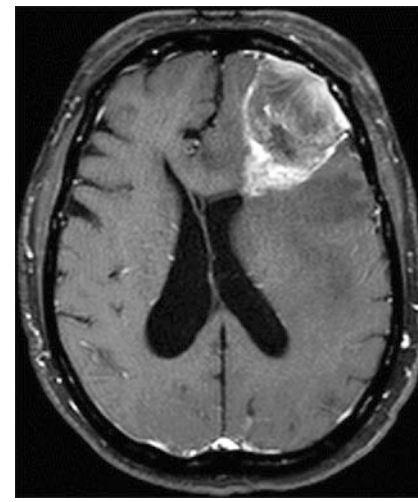

Fig. 1.12 Small cell lung carcinoma metastasis to the brain. The post-contrast T1-weighted MRI in a 40-pack-year smoker who presented with a 2 weeks history of aphasia, forgetfulness, and frequent falls shows a heterogeneously enhancing mass within the left frontal lobe with associated subfalcine herniation

Fig. 1.13 Non-small cell lung cancer brain metastases. The patient has a 40-pack-year smoking history, and known small cell lung cancer metastases to the bone developed altered mental status and intermittent left-sided weakness. The axial post-contrast T1-weighted MRI shows ring-enhancing lesions in the right cerebral hemisphere and a smaller solidly enhancing lesion in the left frontal lobe (*arrow*)

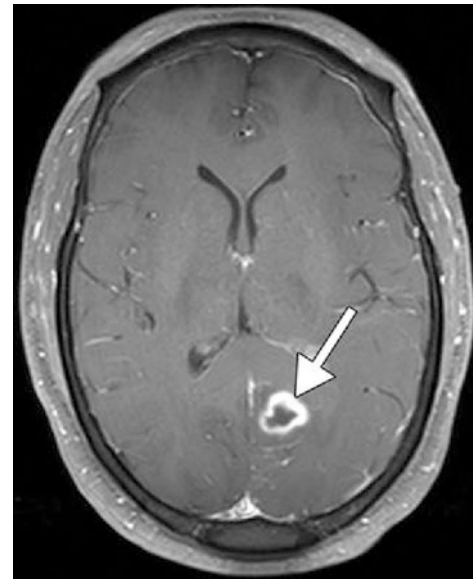

Fig. 1.14 Glioblastoma. Axial post-contrast T1-weighted MR image shows a ring-enhancing mass centered in the left posterior cingulate gyrus (*arrow*)

cancer metastases to the brain are typically iso- to hypointense on T1 and hyperintense on T2-weighted sequences. The enhancement pattern is usually intense whether uniform, punctate, or ring enhancing. Hemorrhagic lung metastases may display high intrinsic T1 signal. On T2-weighted sequences, metastatic lesions are typically hyperintense with hyperintense peritumoral edema. On MR spectroscopy, there is often an intratumoral choline peak without choline elevation in the peritumoral edema and depletion of NAA. CT may be the initial exam obtained when metastatic disease is not yet known. On precontrast imaging, the mass may be iso- to hypoattenuating, surrounded by variable amounts of vasogenic edema. Similar to MRI, following administration of contrast in CT, enhancement is variable and can be intense, punctate, nodular, or ring enhancing. It is also important to evaluate the skull, soft tissues, and head and neck lymph nodes for additional metastases.

The differential diagnosis for brain metastases includes primary brain tumors (Fig. 1.14), cerebral abscess (refer to Chaps. 7, 16, 19, and 46), focal subacute stroke, and tumefactive demyelinating lesions.

1.3.6 Warthin Tumor

Papillary lymphomatous cystadenoma of the parotid gland, or Warthin tumor, is significantly associated with a history of cigarette smoking. Indeed, over 90% of Warthin tumors occur in tobacco smokers. The tumor arises almost exclusively in the parotid gland and has a predilection for male Caucasians. These lesions most commonly present as asymptomatic masses, but may cause facial nerve paralysis or tinnitus. Warthin tumors consist of oncocytic cells containing numerous mitochondria frequently showing structural abnormalities and reduced metabolic function. Smoking can lead to damage to mitochondrial DNA due to the development of numerous reactive oxygen species. In this context, a high rate of deleted mitochondrial DNA

Fig. 1.15 Warthin tumor. This smoker with COPD presented with growing right-sided neck mass. The coronal post-contrast CT image shows a well-defined hyperattenuating mass within the right parotid tail (*arrow*)

has been detected in the oncocytic cells of Warthin tumor. Typical imaging features consist of well-defined solid and/or cystic masses usually within the inferior pole (tail) of the parotid gland, not infrequently multifocal and bilateral (Fig. 1.15).

The differential diagnosis of Warthin tumor includes non-neoplastic conditions, such as benign lymphoepithelial lesions, Sjogren syndrome, and sarcoidosis. For example, benign lymphoepithelial lesions are typically associated with HIV and classically appear as multiple bilateral cystic parotid masses that may contain solid components (Fig. 1.16). Warthin tumors can also resemble pleomorphic adenomas on imaging. However, pleomorphic adenomas are less likely to occur in the parotid tail and display a bosselated appearance and high T2 signal on MRI (Fig. 1.17). While clinical history may be helpful in differentiating some of these possibilities, predictive features of malignancy on imaging include T2 hypointensity of the parotid, ill-defined margins, diffuse growth, infiltration of subcutaneous tissue, lymphadenopathy, and perineural spread (Fig. 1.18). However, Warthin tumors often demonstrate T2 hypointense foci and low ADC values and thus cannot be reliably differentiated from many malignant tumors on diffusion-weighted imaging. In addition, Warthin tumors typically display marked hypermetabolism on ^{18}FDG-PET.

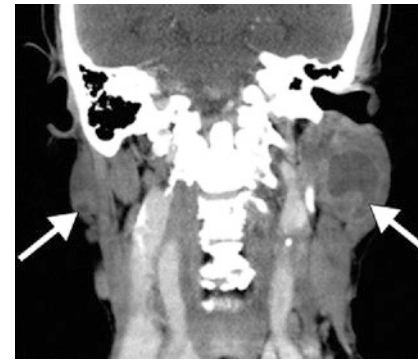

Fig. 1.16 Benign lymphoepithelial lesions in a patient with HIV. The coronal CT image shows cystic lesions in the bilateral parotid glands (*arrows*). The lesion on the left side contains a solid nodule

Fig. 1.17 Parotid pleomorphic adenoma. Axial fat-suppressed T2-weighted MRI shows a bosselated T2 hyperintense mass arising from the deep lobe of the right parotid gland (*arrow*)

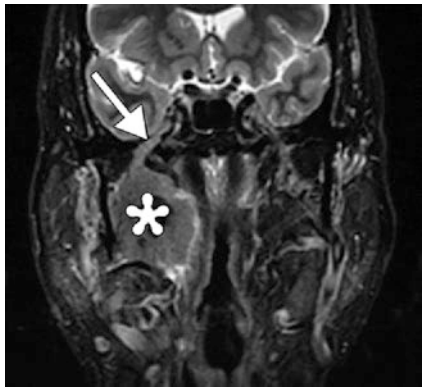

Fig. 1.18 Parotid pleomorphic adenocarcinoma. The coronal STIR MRI shows a heterogeneous mass arising from the deep lobe of the parotid gland with perineural extension along the mandibular nerve across the foramen ovale (*arrow*)

1.3.7 Smoking-Induced Nasopharyngeal Lymphoid Hyperplasia

Heavy tobacco smoking has been linked to the development of nasopharyngeal lymphoid hyperplasia, which is characterized by the presence of cytotoxic lymphocytes in the nasopharyngeal mucosa. The adenoids may be obstructive in up to 30% of heavy smokers. On imaging, there is diffuse symmetric enlargement of the adenoidal tissues (Fig. 1.19). Nevertheless, it is important to exclude other conditions, such as nasopharyngeal carcinoma. In contrast to benign lesions, the configuration of nasopharyngeal carcinoma is often asymmetric, in which the mass is centered

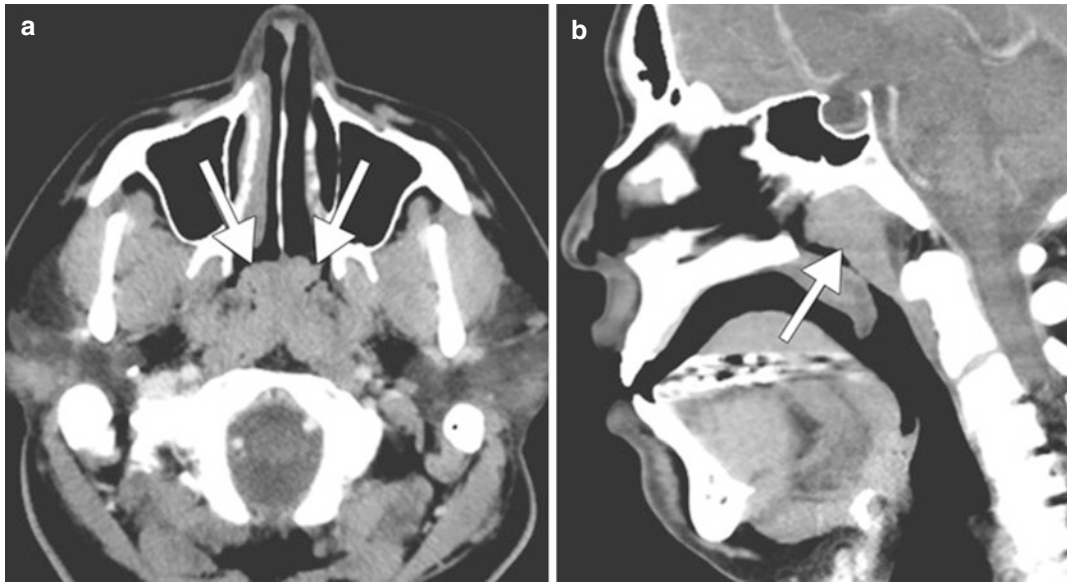

Fig. 1.19 Smoking-induced nasopharyngeal lymphoid hyperplasia. This is a 40-year-old smoker with obstructive symptoms. Axial (**a**) and sagittal (**b**) post-contrast CT images show diffuse marked enlargement of the adenoids (*arrows*)

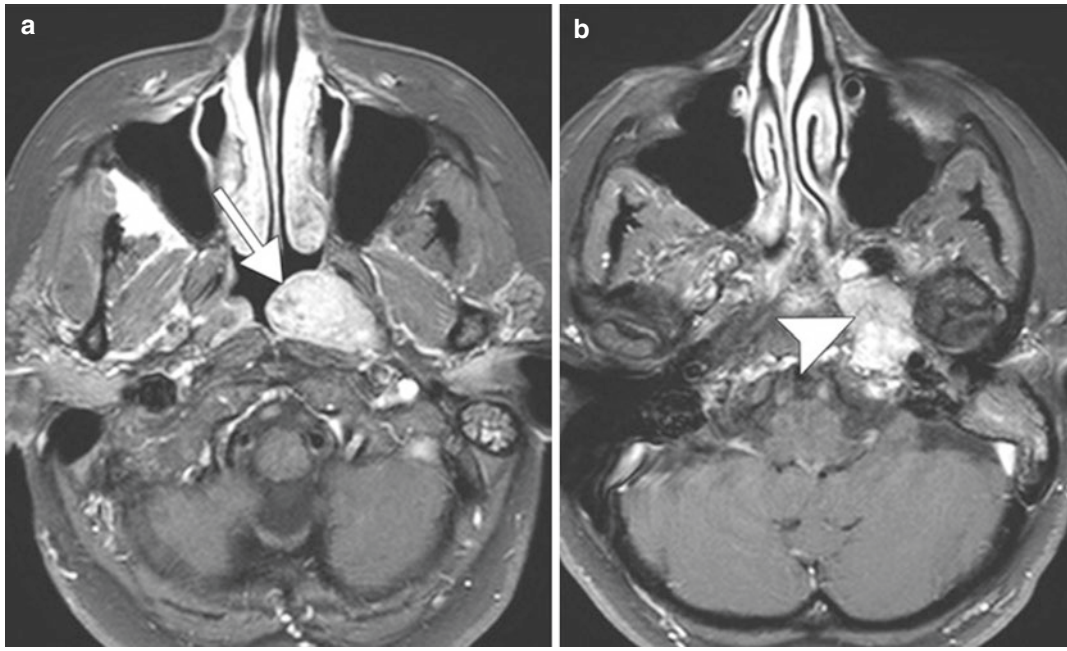

Fig. 1.20 Nasopharyngeal carcinoma. Post-contrast T1-weighted MR images (**a**, **b**) show a bulky mass centered in the left fossa of Rosenmuller (*arrow*). There is associated left skull base invasion (*arrowhead*) and obstructed secretions within the left mastoid air cells

in the fossa of Rosenmuller, and associated with aggressive features, such as skull base invasion (Fig. 1.20). Other differential considerations for smoking-induced nasopharyngeal lymphoid hyperplasia include reactions to other chemical exposures, Epstein-Barr virus infection, and lymphoproliferative conditions.

Suggested Reading

Centers for Disease Control and Prevention. Annual smoking-attributable mortality, years of potential life lost, and productivity losses—United States, 2000–2004. MMWR Morb Mortal Wkly Rep. 2008;57(45):1226–8. Accessed 28 Jun 2014.

Centers for Disease Control and Prevention. QuickStats: number of deaths from 10 leading causes–National Vital Statistics System, United States, 2010. MMWR Morb Mortal Wkly Rep. 2013;62(08):155. Accessed 28 June 2014.

de Ru JA, Plantinga RF, Majoor MH, van Benthem PP, Slootweg PJ, Peeters PH, Hordijk GJ. Warthin's tumour and smoking. B-ENT. 2005;1(2):63–6.

Finkelstein Y, Malik Z, Kopolovic J, Bernheim J, Djaldetti M, Ophir D. Characterization of smoking-induced nasopharyngeal lymphoid hyperplasia. Laryngoscope. 1997;107(12 Pt 1):1635–42.

Galbiatti AL, Padovani-Junior JA, Maníglia JV, et al. Head and neck cancer: causes, prevention and treatment. Braz J Otorhinolaryngol. 2013;79(2):239–47.

Haddad RI, Shin DM. Recent advances in head and neck cancer. N Engl J Med. 2008;359(11):1143–54.

Hashibe M, Brennan P, Benhamou S, et al. Alcohol drinking in never users of tobacco, cigarette smoking in never drinkers, and the risk of head and neck cancer: pooled analysis in the International Head and Neck Cancer Epidemiology Consortium. J Natl Cancer Inst. 2007;99(10):777–89.

Ikeda M, Motoori K, Hanazawa T, Nagai Y, Yamamoto S, Ueda T, Funatsu H, Ito H. Warthin tumor of the parotid gland: diagnostic value of MR imaging with histopathologic correlation. AJNR Am J Neuroradiol. 2004;25(7):1256–62.

Juvela S. Prevalence of risk factors in spontaneous intracerebral hemorrhage and aneurysmal subarachnoid hemorrhage. Arch Neurol. 1996;53:734–40.

Juvela S, Hillbom M, Numminen H, Koskinen P. Cigarette smoking and alcohol consumption as risk factors for aneurysmal subarachnoid hemorrhage. Stroke. 1993;24:639–46.

Juvela S, Porras M, Poussa K. Natural history of unruptured intracranial aneurysms: probability of and risk factors for aneurysm rupture. J Neurosurg. 2000;93:379–87.

Juvela S, Poussa K, Porras M. Factors affecting formation and growth of intracranial aneurysms: a long term follow up study. Stroke. 2001;32:485–91.

Longstreth WT Jr, Nelson LM, Koepsell TD, van Belle G. Cigarette smoking, alcohol use, and subarachnoid hemorrhage. Stroke. 1992;23:1242–9.

Ockene IS, Miller NH. Cigarette smoking, cardiovascular disease, and stroke: a statement for healthcare professionals from the American Heart Association. Circulation. 1997;96(9):3243–7. Accessed 28 Jun 2014.

Raval M, Paul A. Cerebral venous thrombosis and venous infarction: case report of a rare initial presentation of smoker's polycythemia. Case Rep Neurol. 2010;2(3):150–6.

Schuette W. Treatment of brain metastases from lung cancer: chemotherapy. Lung Cancer. 2004;45(Suppl 2):S253–7.

Tonini G, D'Onofrio L, Dell'Aquila E, Pezzuto A. New molecular insights in tobacco-induced lung cancer. Future Oncol. 2013;9(5):649–55.

U.S. Department of Health and Human Services. Reducing the health consequences of smoking: 25 years of

Alcohol

2

Michael C. Veronesi and Daniel Thomas Ginat

2.1 Uses

Alcoholic beverages are commonly consumed for pleasure and a form of stress reduction since at least the Neolithic period many thousands of years ago. The beverages are produced through the fermentation of various fruit juices and grains. Alcohol can provide an increased sense of self-confidence, disinhibition, mild euphoria, and decreased anxiety but also impaired judgment and attention span, even with low blood levels. There are a few reported health benefits associated with low to moderate alcohol consumption, such as reduction of cardiovascular disease risk factors. Nevertheless, alcohol is one of the most commonly abused substances, and alcohol dependence is a major cause of disease burden. Alcohol in the form of ethanol can be used for sclerotherapy, but this is beyond the scope of the chapter.

2.2 Mechanism

The alcohol found in beverages is ethanol or ethyl alcohol (C_2H_6O). Alcohol metabolism is a complex process with large variations between individuals that are mainly related to genetic factors. Direct absorption of alcohol into the bloodstream occurs in the stomach and small intestine. The liver metabolizes nearly 90% of alcohol. Alcohol dehydrogenase oxidizes ethanol into acetaldehyde, which is then further oxidized into acetic acid by acetaldehyde dehydrogenase, and finally into carbon dioxide and water through the citric acid cycle. The effects of alcohol upon the central nervous system can be either direct or indirect. The main direct effect of alcohol is volume loss due to neurotoxicity, often mediated by a compromise of neurotransmitters and/or receptors and electrolytes. Conversely, indirect effects are related to liver cirrhosis, such as hepatic encephalopathy and coagulopathies, and impaired vitamin absorption. In some conditions, it is unclear whether direct or indirect effects or a combination thereof is responsible, such as Wernicke encephalopathy, osmotic myelinolysis, and Marchiafava-Bignami disease.

2.3 Imaging Findings

Marchiafava-Bignami disease: Marchiafava-Bignami disease is a rare condition that mainly affects chronic alcoholics, particularly middle-aged males, and results in progressive demyelination and necrosis of the corpus callosum. Patients present acutely with mental confusion, disorientation, neurocognitive deficits, and seizures, generally ensued by coma and death. On

M. C. Veronesi · D. T. Ginat (✉)
Department of Radiology, University of Chicago, Chicago, IL, USA
e-mail: dtg1@uchicago.edu

© Springer Nature Switzerland AG 2022
D. T. Ginat et al. (eds.), *Neuroimaging Pharmacopoeia*,
https://doi.org/10.1007/978-3-031-08774-5_2

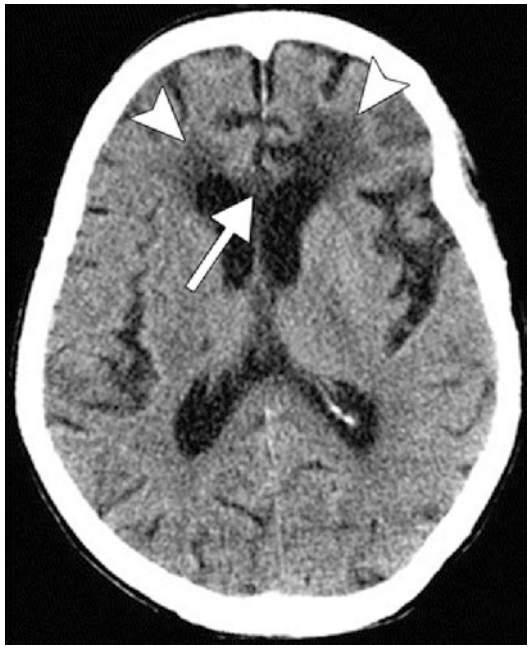

Fig. 2.1 Marchiafava-Bignami disease depicted on CT. Axial non-contrast CT shows hypoattenuation in the genu of the corpus callosum (*arrow*) and adjacent periventricular white matter (*arrowheads*)

CT, diffuse periventricular hypoattenuation associated with focal areas of hypoattenuation in the splenium and sometimes the genu of the corpus callosum can be observed (Fig. 2.1). On MRI, the affected areas display T2 hyperintensity and variable degrees of restricted diffusion and enhancement depending on the severity and acuity of the disease (Fig. 2.2). In fact, apparent diffusion coefficient restriction of the corpus callosum and cortical lesions were associated with a higher mortality rate and a more severe cognitive impact. MR spectroscopy may reveal decreased NAA-Cr ratio and elevated lactate during the first few months of the disease process. Chronic lesions appear cystic and well marginated. Lesions of the corpus callosum that may have a similar appearance to Marchiafava-Bignami disease include other demyelinating processes, infarction, viral encephalitis, metronidazole (refer to Chap. 28), antiseizure medications (refer to Chap. 33), and shearing injuries (Fig. 2.3).

Traumatic brain injury and hemorrhage related to alcohol: Traumatic brain injury (TBI) is a serious public health problem in the USA. Each year, at least 1.7 million traumatic brain injuries occur and contribute to substantial morbidity and mortality. Preexisting alcohol abuse is common among persons who incur TBI, with as many as 58% reporting a history of alcohol abuse or dependence and as much as 25% reporting previous treatment for substance abuse in one study. In a separate study analyzing 2657 trauma patients experiencing TBI, 58% had a heavy drinking history, 46% had a positive blood alcohol level at the time of injury, and 36% were intoxicated. Alcohol intoxication resulted in a greater likelihood of intubation, intracranial pressure monitoring, respiratory distress, and pneumonia. Timely management of TBI can significantly alter the clinical course if detected with neuroimaging within 48 h of the injury. Clinical manifestations that suggest major injury such as worsening level of consciousness, loss of consciousness for more than 5 min, focal neurological findings, seizure, failure of the mental status to improve over time, signs of a basal or depressed skull fracture, or confusion on examination almost always merit imaging. Conversely, even patients with absence of clinical findings and high-risk circumstances can have intracerebral hemorrhage on imaging. Neuroimaging also plays an important role in the diagnostic workup of TBI. MRI is superior to CT in detecting axonal injury and cerebral contusions. However, conventional CT generally remains the initial imaging modality of choice during the first 24 h following injury. Alcohol intoxication can lead to severe injuries related to high-speed motor vehicle collisions while driving intoxicated or falls related to drunkenness, resulting in skull fractures, intracranial hemorrhage, cerebral contusions, and shear injury (Figs. 2.3 and 2.4). Alcoholism may also predispose to large and recurrent intracranial hemorrhage with relatively minor trauma due to underlying coagulopathy related to hepatic dysfunction (Fig. 2.5). Alcohol abusers also have a tendency to engage in violent behavior when

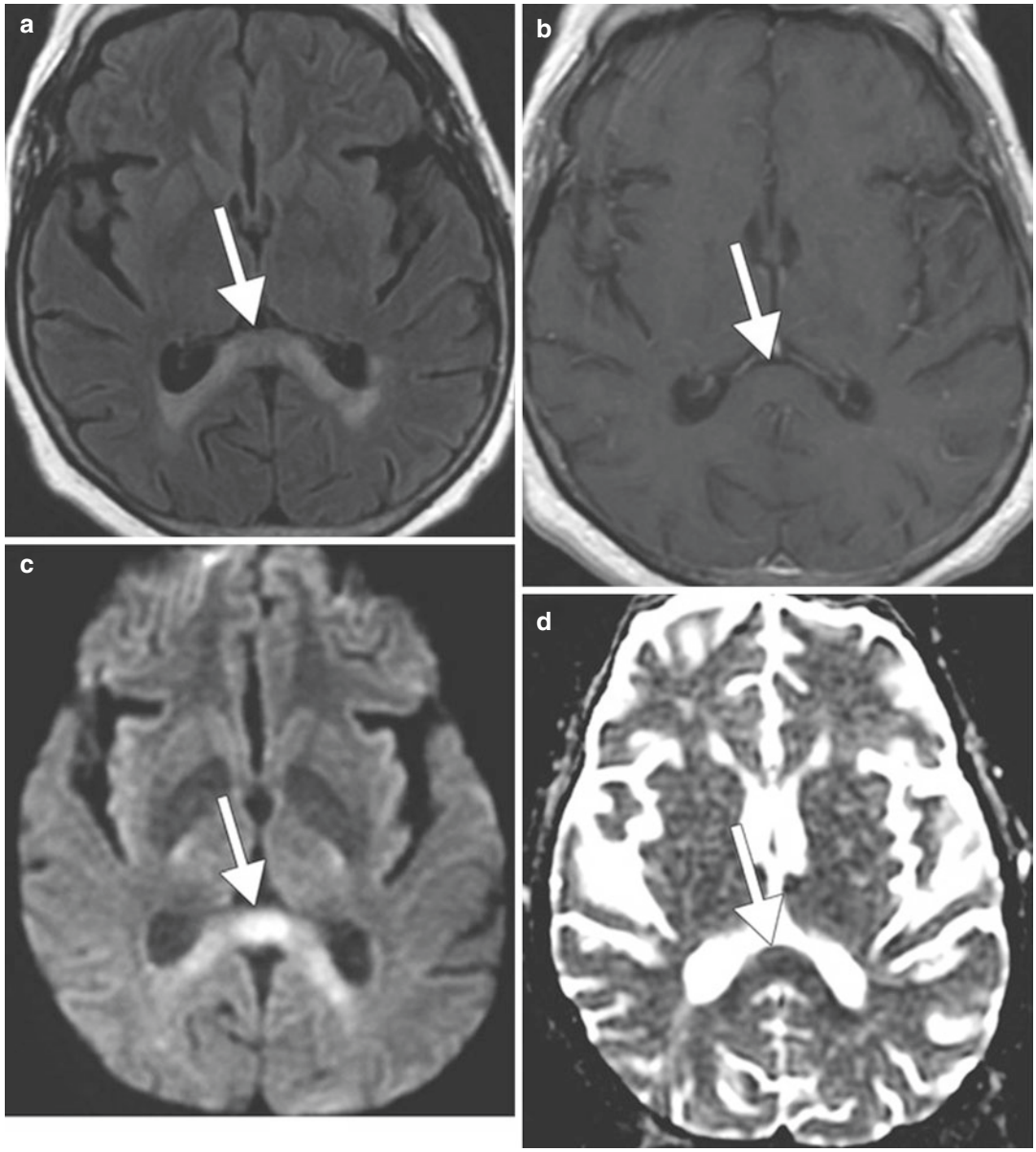

Fig. 2.2 Marchiafava-Bignami disease depicted on MRI. Axial T2-weighted FLAIR MRI (**a**), post-contrast T1-weighted MRI (**b**), DWI (**c**), and ADC map (**d**) show non-enhancing T2 hyperintensity in the splenium of the corpus callosum (*arrows*)

drunk and may present with maxillofacial fractures, for which CT may be obtained (Fig. 2.6). Incidentally, these individuals often have a high burden of dental disease that may also be encountered on imaging.

Hepatic encephalopathy (also refer to Chaps. 34, 55, and 58*)*. Hepatic encephalopathy (HE) may occur as an acute, potentially reversible disorder, or it may occur as a chronic, progressive disorder that is associated with chronic liver dis-

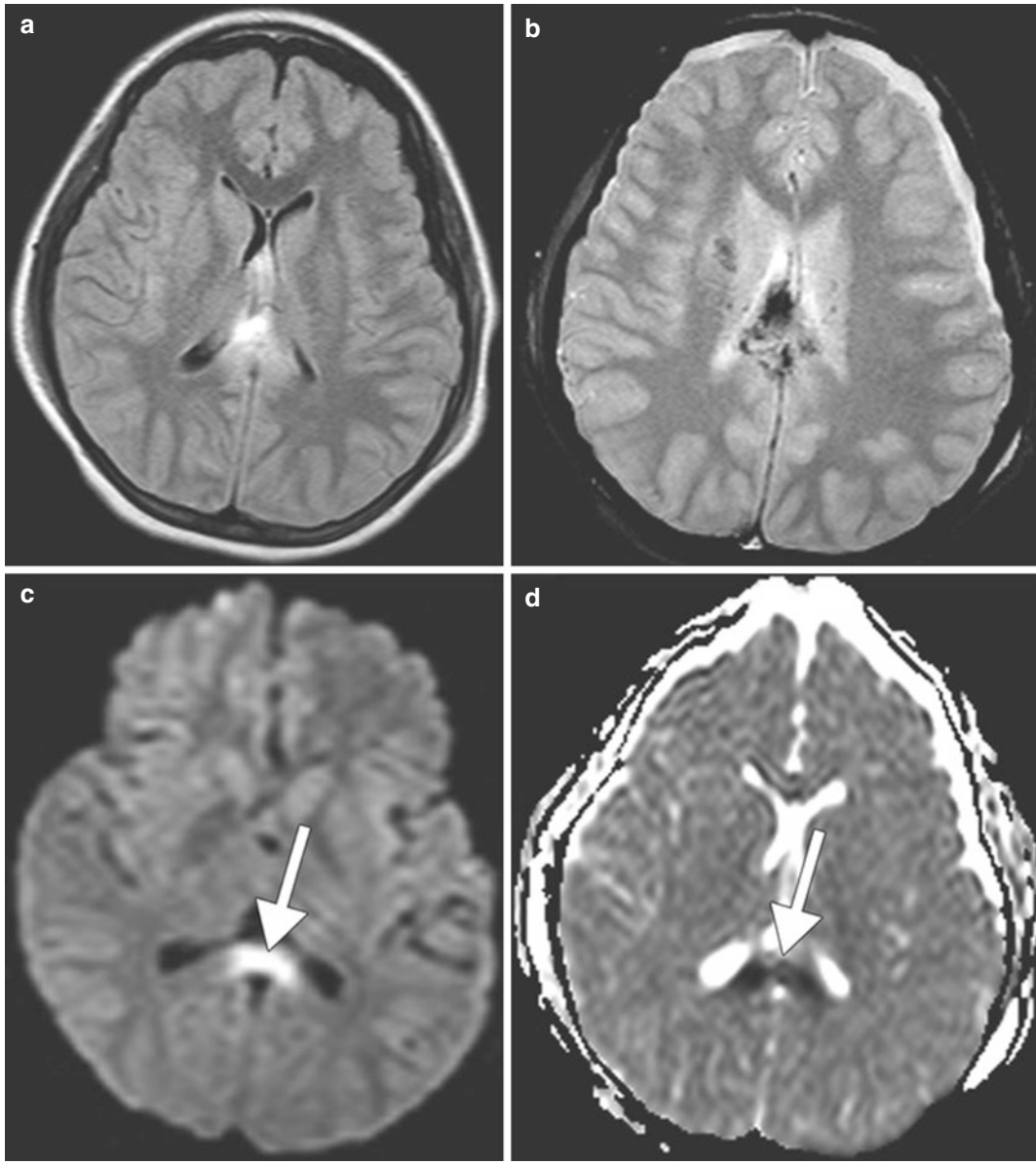

Fig. 2.3 Shear injury. The patient has a recent history of severe trauma to the head. Axial T2-weighted FLAIR MRI (**a**), T2* GRE (**b**), DWI (**c**), and ADC map (**d**) show edema and hemorrhage within the corpus callosum with associated restricted diffusion in the splenium of the corpus callosum (*arrows*)

ease. Depending on the duration and extent of hepatic dysfunction, HE may be classified into fulminant hepatic failure (acute) or portosystemic encephalopathy (chronic). Clinical manifestations of HE can range from mild confusion to coma. Cerebral edema and raised intracranial pressure can result from fulminant hepatic failure and contribute to encephalopathy, but some degree of cerebral edema has been shown in patients with all grades of hepatic encephalopathy. Patients with the portosystemic encephalopathy frequently have pairs and triplets of abnormal astrocytes with a characteristic structure known as Alzheimer type II astrocytosis, in which the astrocytes exhibit physiological and functional abnormalities. When the liver is damaged, either

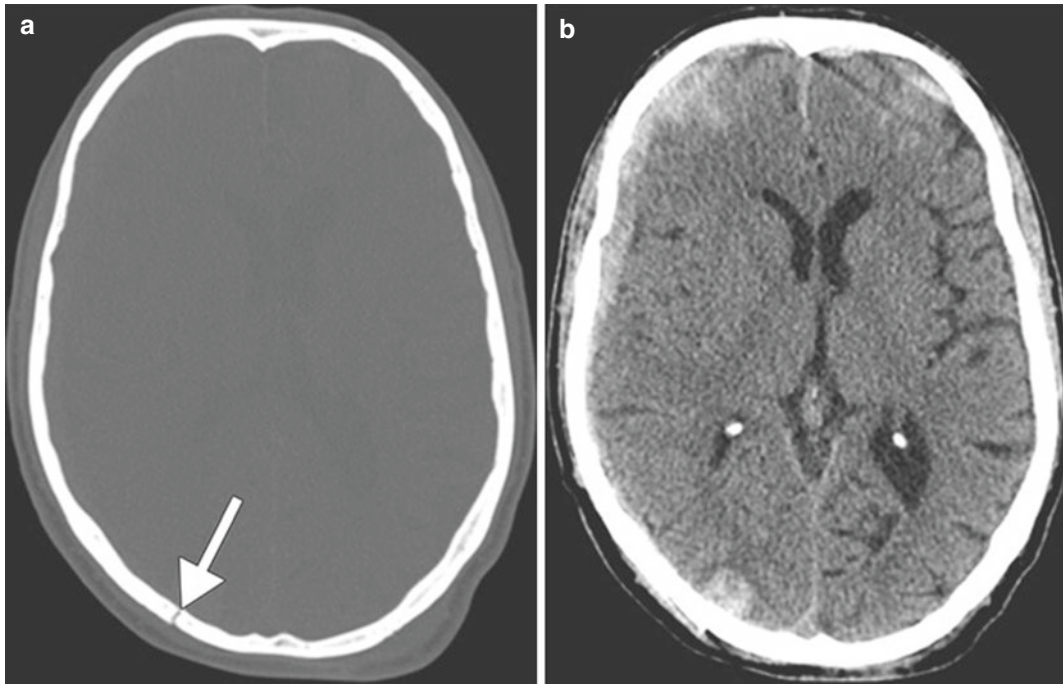

Fig. 2.4 Alcohol-related traumatic brain injury. Axial CT images in the bone (**a**) and brain (**b**) windows show a non-depressed right occipital bone fracture (*arrow*) and scattered acute intraparenchymal hemorrhage, including a right cerebral convexity subdural hematoma, subarachnoid hemorrhage, and hemorrhagic contusions in a patient who fell while drunk

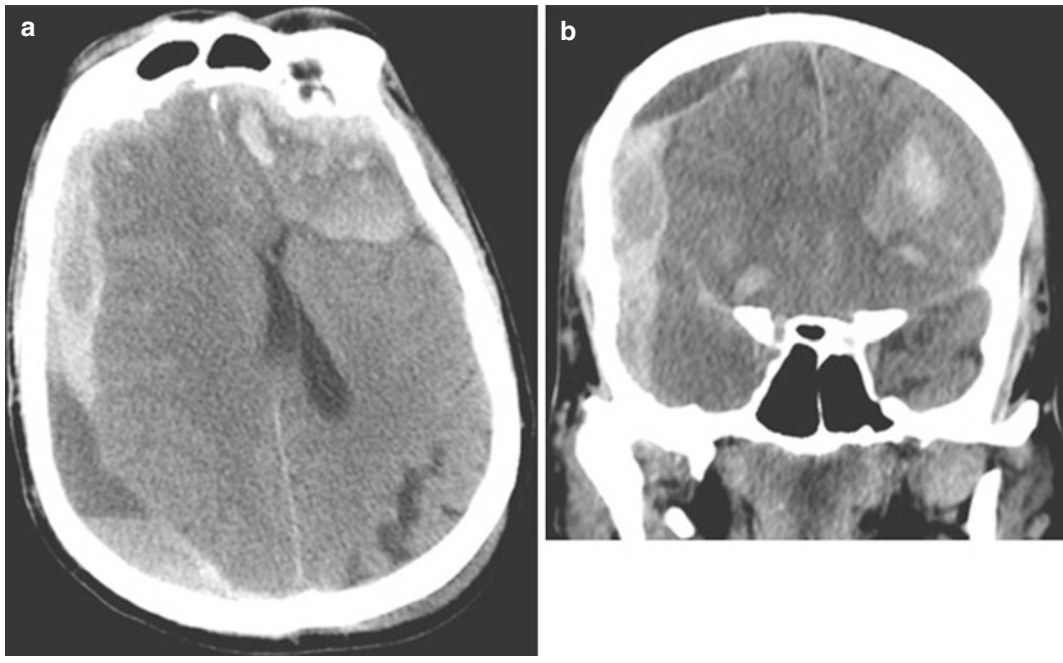

Fig. 2.5 Acute upon chronic intracranial hemorrhage in a patient with alcohol-induced hepatic coagulopathy. Axial (**a**) and coronal (**b**) show a heterogeneous acute upon chronic right cerebral convexity subdural hematoma and a left frontal lobe hemorrhagic contusion and areas of subarachnoid hemorrhage in a patient with alcohol-induced liver failure and trauma